

Dynamic Walking and Stepping over Large Obstacles of Biped Robots: A Poincaré Map Approach

Nasrin Kalamain^{1,*} and Mohammad Farrokhi²

¹School of Electrical Engineering, Iran University of Science and Technology, Tehran, Iran

²School of Electrical Engineering, Center of Excellence for Modeling and Control of Complex Systems, Iran University of Science and Technology, Tehran, Iran

Received 17 March 2022; Accepted 7 December 2022

Abstract

This paper considers dynamic stepping of biped robots when walking through a big obstacle, which is a great problem for these kinds of robots, using nonlinear model predictive control technique. No need for trajectory planning is one of the key advantages of this method. Hence, the gait length is not predefined and the controller determines it on the basis of the physical restraints and dynamic constancy conditions for approaching the obstacle and stepping over it. The stability and good performance for stepping over large obstacles are guaranteed by the definition of appropriate linear and nonlinear constraints and cost functions. Furthermore, to solve the uncertainty problem corresponding to the biped dynamic model, neural networks are used to identify the model of robot. For stability analysis, the Poincaré map with the fixed-point technique is utilized to guarantee the robot stability. Simulation outcomes indicate excellent efficiency of the suggested technique used to a five-link biped robot crossing over a 40×15 cm obstacle in sagittal plane when preserving a safety clearance from it with no need to a predefined trajectory.

Keywords: Biped Robots, Nonlinear Model Predictive Control, Neural Network, Poincaré Map, Fixed Point.

1. Introduction

Mechanical biped locomotion has been studied for over past 30 years. Legged robots are able to step in unidentified, irregular, rough and sloppy grounds. They are able to cross through obstacles or pass over channels and go up and down the stairs; while wheeled robots cannot perform these tasks. These new needs along with the new concepts in the biped robots field (e.g., suggesting steady stepping and maintaining balance to the biped robot) demand using novel and well-adapted motion control methods [1].

Many of the proposed control approaches in the studies of walking of biped robots are based on trajectory tracking and reducing the tracking error by designing a gait planner. However, human walking is not based on a predefined route because defining a trajectory and making efforts to follow it may not yield natural walking, especially when there are obstacles on the way. Generally, predefined or off-line route planning is relatively easy to perform but has some characteristic limitations. Firstly, the route must be adapted for the robot in hand. Therefore, all robots need their own route. Secondly, different routes must be designed for diverse lands. Third, a predefined route may not look like human stepping. Hence, a legged robot may have a standard and adequate walk even if there are several errors in the route tracking of the connections. According to these ideas, in [2], the authors have planned a route-free motion control of bipeds on the basis of the Nonlinear Model Predictive Control (NMPC). They have taken into account several physical and valuable restraints for static stepping at flat lands. Though, the problem in this technique is that the robot walks very slowly. In [3], the MPC has been utilized for dynamical walking of HRP-2 as a humanoid robot. In his technique, the objective

function reduces the off-line error between the desired and real Zero Moment Point (ZMP) to its minimum value. The MPC has been applied to generate on-line routes and controlling the robot simultaneously [4]. In this technique, by taking into account the physical restrictions of the robot, an optimum path and control technique is formed. In [5], the gait length is not constant and the robot's stepping is as same as human stepping but it walks slowly. The NMPC utilizes the dynamic model of the robot for forecast. Therefore, the prediction model is not very accurate due to the model uncertainties. Hence, authors have utilized nonlinear disturbance observer to solve this problem.

The distributed MPC method is offered to guarantee postural constancy of a biped robot in the presence of big external disturbances [6]. The simulation results, performed on iCub biped robot, show effectiveness of the suggested technique. In [7], the NMPC is utilized for determination of the next footstep position of a humanoid robot in existence of strong external turbulences. The experimental outcomes on LOLA humanoid robot indicate excellent performance of the suggested technique. In [8], the LMPC is used to generate on-line trajectory for biped walking based on the three-mass with angular momentum model. It is claimed that the three-mass with angular momentum model decreases the modeling and ZMP tracking errors. The simulation outcomes and observations show the performance of the recommended technique on a 5-DOF biped robot. The controlled nonlinear optimization problem is applied to control a biped robot for crossing wide ditches [9, 10]. The ditch width is higher than or equal to the length of the leg. The limitation on the angular velocities and joint actuator torques are defined as restraints of the optimization problem. The simulation outcomes on a seven link planar biped robot indicate excellent performance of the suggested technique.

*E-mail address: nkalamian@ee.kntu.ac.ir

ISSN: 1791-2377 © 2022 School of Science, IUT. All rights reserved.

doi:10.25103/jestr.156.23

In [11], an on-line suppression of the bifurcation gait is presented for a 3-DOF biped robot based on model predictive controller. The robot constancy is assured utilizing Poincaré map. Simulation outcomes display excellent efficiency of the suggested technique in disturbance rejection. A dynamic stepping pattern generator according to the model predictive control is suggested for a 29-DOF humanoid robot DRC-HUBO+ [12]. The MPC is used to adjust footsteps and recover balance under external disturbances. The outcomes show good efficiency in ZMP maintenance within support polygon during strong perturbation. The MPC is employed for online gait generation for humanoid robots on uneven surfaces [13]. Furthermore, in [14], the MPC is utilized to control biped robot with bounded uncertainties. In [15], a ZMP variation based on body acceleration is subjected for disturbance rejection in biped robots. Furthermore, a high-order extended state observer (ESO) is utilized for disturbance rejection in biped robots [16]. The ESO estimates disturbance signal as an unknown input; then, the controller can compensate it based on the estimated value. The stability of suggested technique is provided by the Lyapunov theory. The numerical outcomes indicate the good performance of the presented method in comparison with high-order sliding-mode observer under the same disturbances.

Walking through obstacles is a serious challenge for the biped robot because when its legs get up, the stability is strongly at risk. Therefore, it is difficult to control a biped robot to pass barriers while holding its balance. Because of this problem, nearly all studies in this field have considered short barriers. There exist famous robots with the ability to walk over small obstacles. As it was mentioned, previous investigations on walking over barriers have predefined trajectories for the swinging leg tip and the robot's hip. Then, the control of biped is performed to trace these predefined pathways. In [17], the authors have suggested a technique for HRP-2 humanoid robot. In their technique, an algorithm discovers possible conditions for walking over a barrier. If the response is yes, the robot utilizes the predefined off-line route and passes through the barrier. The robot senses the objectives and chooses the best predefined route based on an algorithm. Then, the control of robot is performed using the ZMP stability criterion. In [18], for walking through obstacles, the authors have suggested a technique to preserve the projection of the Center of Mass (COM) of the robot in the supporting polygon area that can assure static stability. However, the HRP-2 robot steps over obstacles very slowly because of the static movements of the robot. They have utilized the ZMP measures to maintain the robot's dynamic stability. In [19], the authors have suggested a technique for HRP-2 (30-DOF, 165cm) robot that can over a 25×5cm obstacle. A decentralized control technique has suggested on the basis of the fuzzy logic for passing over a 5cm obstacle for a small humanoid robot (55cm, 21-DOF) [20]. The motion trajectory for crossing over small obstacles has designed off-line and the fuzzy controller has employed to guarantee robot balance with torso gesture. The HR moves its legs over the obstacle and after each step, changes the torso position to keep its balance. This routine makes its motion very slow. In [21], an off-line gait designing strategy is proposed for an 18-DOF humanoid robot named BIOLOID. The authors use forward and inverse kinematics formulations and find a suitable gait for the robot in sixteen different steps to cross over obstacles without any collision. The gait designing is based on the Center of Pressure (COP) and COM tracking technique. The motion planning consists of kinematics solutions. The interpolation formulations are designed to generate a

trajectory for a 21-DOF humanoid robot named Bonten-Marui II [22]. In this strategy, the robot can sense a wall surface and correct its locomotion direction, avoids large obstacles and steps over small obstacles. In [23], the event-based control method is utilized to control Lola humanoid robot for climbing stairs and overcoming small obstacles. Moreover, a vision-based control is presented for humanoid navigation utilizing virtual memory with obstacle avoidance [24].

The biped robots are subject to several uncertainties in their dynamics such as weight variations, joint frictions, etc. Moreover, there are several unmodeled dynamics in the model of these robots. Furthermore, external disturbances may exist that can make the robot unstable. Therefore, an obvious feature of the biped motion controller is its robustness. One of the solutions for this limitation is modelling the biped robot using intelligent methods such as fuzzy logic or Neural Networks (NNs). The CMAC NNs have been employed for overcoming the problem of uncertainties in a biped robot with 5-DOF [25]. Radial-Basis Function (RBF) NNs has been utilized to identifying the biped robot dynamic model [26]. The objective was to numerically calculate the Jacobian matrix that is needed in the control algorithm. Moreover, in [27], reinforcement learning and neural network are employed for gait generation of a humanoid robot.

The stability test is one of the main and difficult concepts in the area of the biped robots. The Poincaré return map is a suitable method for analyzing periodic dynamic systems such as biped robots. The advantage of this method is that it decreases the analysis of the periodic orbits to the analysis of the equilibrium points (fixed points). However, the main challenge in using the Poincaré method is finding a closed-form solution of the return map, which is almost impossible for highly nonlinear systems. Numerical schemes can be utilized to calculate the return map and find its fixed points. In this way, eigenvalues can be used to determine the stability. However, numerical calculations are typically time intensive and doing them iteratively as part of a system design procedure can be hard. Moreover, numerical computations are not perceptive in the sense that it is difficult to alter the controller based on the stability features of the fixed point of the Poincaré map.

Grizzle et al. have analyzed a simple biped robot (3-DOF) stability during 2-D walking by Poincaré method and periodic orbits [28]. The reference route of stepping has been designed off-line. The complexity of dynamic model for the biped robot, leads to stability proof problems. Therefore, for reducing these difficulties, dynamic model is considered under-actuated that reduces the order of the dynamic equation to two (zero dynamic). Also for simplifying, only the SSP and impulse phases have been considered. The authors have improved their strategy and designed a control law on the basis of the Poincaré map for asymptotically stable walking of their simple under-actuated biped robot [29]. This law has been computed based on the robot dynamic model. They also have determined some virtual constraints for the motion planning and have indicated that the zero dynamic stability guarantees the complete model stability. The virtual limitations are holonomic limitations on the configuration of robot that are asymptotically achieved using a feedback controller.

In [30], the authors have utilized a simple 3-DOF biped robot with central pattern generator (CPG) method to control it. The robot moves using a rhythmic signal from an oscillator, which takes feedback signals from the touch sensors at the legs' tips. According to such a simple model, estimated

periodic solutions are achieved and the stepping stability is analytically studied using the Poincaré map. Furthermore, this map is utilized for the passive dynamic walking of the extent-step biped robot [31]. In light of the experiments on RABIT and in preparation for a new robot called MABEL, Morris has developed extensive new design tools that addresses the performance limitation aspects of the previous hybrid zero-dynamic (HZD) controllers [32]. In conjunction with deriving smooth stabilizing controller, Morris has presented two new sets of hypotheses under which the reduced-dimension Poincaré map can be utilized for low dimensional stability tests. Grizzle et al. have applied this technique for a 6-DOF 3D biped robot in [33]. By considering three important variables that have direct effect on the stability, analysis is limited from six to three degrees. Using linearization of the Poincaré map (the Jacobian matrix), Authors have shown that it is possible to find the eigenvalues and the test stability. In [34], two stiffness control methods including torque balance and surface fitting are used for a biped robot. In [35], for online path planning, a hybrid fast marching approach is utilized for biped robots. Poincaré map is subjected to investigate the local stability of a biped robot controlled by a PD [36].

In [37], the NMPC is employed to control a biped robot for passing over barriers without any demand for off-line trajectories. Then, the idea was extended by using neural networks as the dynamic model of the robot for the NMPC [38]. The NMPC has also been used for biped robots to climb up and down the stairs with on-line trajectory generation [39].

Most of the aforesaid articles have utilized off-line paths for walking or passing over barrier. However, some papers focus on designing an on-line trajectory [3, 4]. In these papers, reference trajectories for legs and torso is calculated on-line and then controller tries to track them. As it is obvious, this approach is more adaptive than the off-line trajectory. Nevertheless, a desired trajectory has to be produce first. If the trajectory generation is removed from the control process, the biped can adapt itself better to the environment especially when some obstacles that are not know to the controller a priori, appear on the walk path of the robot. This paper eliminates the need for predefined trajectories for the biped robots. To this end, the proposed method employs the NMPC for a synchronous on-line path planning and controlling of the robot. Some scientists utilized the MPC to achieve off-line optimal trajectories for the biped robots. However, their method is not as good as a free-trajectory technique that is the main contribution of this manuscript. Moreover, a few articles have employed MPC for on-line path planning [2, 5]. Nevertheless, none of them has considered crossing over big obstacles, which is a challenging problem and is considered in this paper. In most articles, the obstacle is so small that the robot barely raises its legs as if no obstacle exists. Consequently, it is easier to assurance a stable walking. In contrast, in the suggested algorithm in this manuscript, a large barrier is investigated that makes the dynamic stability of the robot a big challenge. Furthermore, a usual problem in the aforementioned papers is that the gait length is kept fixed meaning the robot must reach the obstacle at a certain and predefined point, which is not possible in all practical cases. Moreover, maintaining a fixed gait length can decrease the robustness of the control technique against external turbulences. In contrast, in our proposed method, the NMPC changes the gait length to provide more stability to the controller when unexpected external disturbances incur. Moreover, it can add more flexibility to the robot, particularly when the robot is approaching a large obstacle and attempting

to go over it. Hence, the gait length is not considered constant and the robot can walk and stop near the barriers. One important point is that the MPC methods are model-based schemes that can cause a difficulty when uncertainties occur in the robot model, which can happen popularly in practical situations. In current study, NNs are utilized for providing a better generalized model to the NMPC. For stability analysis of the NMPC, the Poincaré map is employed. This can be compared with the previous studies, where off-line trajectory is created for assessment of the tracking error and the constant point of the Poincaré map. Hence, the constant point in the proposed method should be found experimentally. With linearization of the Poincaré return map nearby the constant point and computation of the Jacobian matrix, the eigenvalues are found and the closed-loop system is investigated in terms of the stability. It is worth to be mentioned, NMPC without offline trajectory for dynamic walking and stepping over obstacles has not been presented in any research in this area before.

The present paper is organized as follows. Section 2 introduces dynamic model for the robot. The NMPC controller structure, the cost functions, and the constraints for stepping and passing over barriers will be presented in Section 3. Section 4 presents the neural network for the model identification. The stability test using the Poincaré map is described in Section 5. Section 6 represents simulation outcomes followed by conclusion in Section 7.

2. Dynamic Model of Biped Robot

Fig. 1 shows the biped robot utilized in this manuscript. This biped includes a torso and two similar lower limbs, which have a thigh and a shank. Furthermore, it has one hip joint, two knee joints, and two ankles at tips of the lower limbs. There is an actuator situated at every joint, which are moving in the sagittal plane. It is assumed that the feet do not have mass. One step of the robot comprises of three stages: 1) Double Support Phase (DSP), 2) Single Support Phase (SSP), and 3) SSP impact. The DSP occurs when both legs are on the ground. The friction between the feet and the ground is supposed adequate to prevent slippage over stepping. The SSP occurs when only one leg (named the supporting leg) is on the ground. These steps will be considered in the followings.

2.1. Single Support Phase

The biped locomotion with a single foot on the ground can be taken into account as an open-loop kinematic chain model [26]. The standard Lagrangian method can be utilized to derive the biped SSP for describing dynamic equations as

$$\mathbf{D}(\boldsymbol{\theta})\ddot{\boldsymbol{\theta}} + \mathbf{h}(\boldsymbol{\theta}, \dot{\boldsymbol{\theta}})\dot{\boldsymbol{\theta}} + \mathbf{G}(\boldsymbol{\theta}) = \mathbf{T} \quad (1)$$

where $\mathbf{D}(\boldsymbol{\theta})$ refers to a 5×5 positive definite and symmetric matrix of inertia, $\mathbf{h}(\boldsymbol{\theta}, \dot{\boldsymbol{\theta}})$ represents a 5×5 matrix associated with the centrifugal and Coriolis terms, and $\mathbf{G}(\boldsymbol{\theta})$, \mathbf{T} , $\boldsymbol{\theta}$, $\dot{\boldsymbol{\theta}}$, and $\ddot{\boldsymbol{\theta}}$ refer to 5×1 vectors of gravity terms, the joints torque vector, the generalized angular position, and the velocity and acceleration of joints, respectively [26].

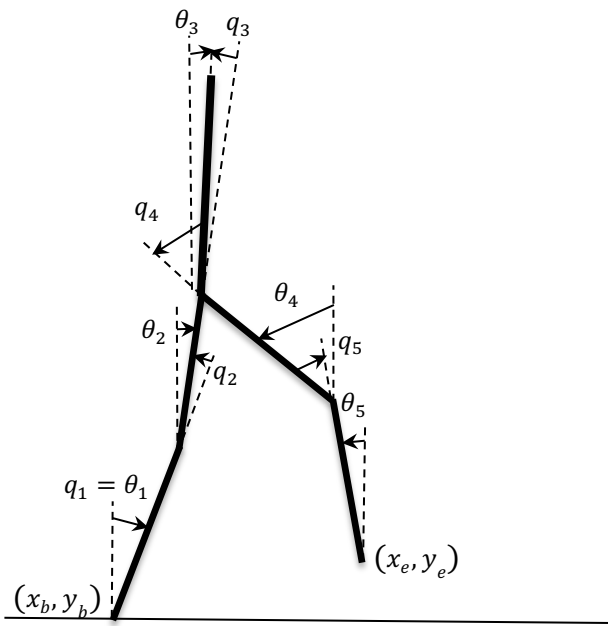


Fig. 1. Five link biped robot

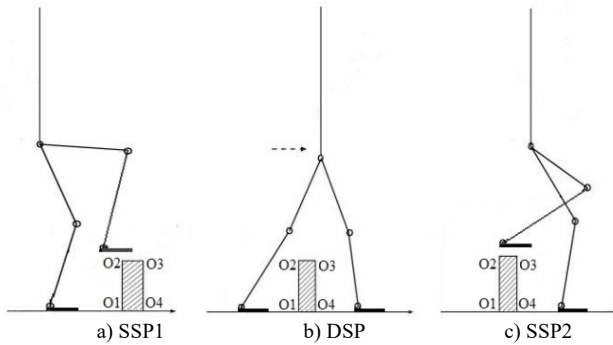


Fig. 2. Crossing over obstacles

2.2. Double Support Phase

The DSP initiates with touching the ground by the front limb and ends when the rear limb takes off the ground. As both of the contact points between the lower limbs and the ground are fixed during the DSP, there exists a set of holonomic constraints. Using the Lagrangian formulation of motion, the dynamic equation in this phase can be represented as

$$D(\theta)\ddot{\theta} + h(\theta, \dot{\theta})\dot{\theta} + G(\theta) = T + J^T(\theta)\lambda \quad (2)$$

where $J(\theta)$ and λ are 5×2 Jacobian matrix and 2×1 vector of Lagrange multipliers, respectively [26].

2.3. Single Support Phase Impact

The robot puts its swinging leg on the ground when the SSP ends. However, there is an immediate effect between the ground and the foot tip. In the present manuscript, it is supposed that the impact only influences the angular velocity. If the impact is big, then the angular position and velocity may incur large momentum to the robot, resulting in instability. Therefore, the control technique should generate as small impact as possible. The angular velocity suddenly right following the contact is

$$\dot{\theta}_{\text{impact}}^+ = \dot{\theta}^- + D^{-1}J^T[J D^{-1}J^T]^{-1}(-J\dot{\theta}^-) \quad (3)$$

where $\dot{\theta}_{\text{impact}}^+$ and $\dot{\theta}^-$ refer to 5X1 angular velocity exactly following and prior the impact, respectively [26].

2.4. Stepping over Obstacles

Walking over an obstacle includes three steps: 1) one leg passes over the obstacle (SSP1), 2) the torso moves forward (DSP), and 3) the back leg crosses over the obstacle (SSP2). These steps are represented in Fig. 2.

3. Nonlinear Model Predictive Controller

In general, the robots motion control comprises of two steps: 1) motion scheduling and 2) route tracking. In biped robots, the motion scheduling (i.e. the gait formation) phase may be carried out off-line or on-line [3]. The off-line gait formation cannot adjust to the environment variations such as obstacles. There are diverse approaches for the on-line gait formation that can adapt to the environment. An on-line and adaptive optimum gait generator would ease best the biped robot movement control. Though a large number of control problems are aimed to do more attempt to reduce the tracking error. However, for the biped walking, perfect joint route tracking is not needed because these robots may have natural walking even if there are some acceptable tracking errors in the joints. Nevertheless, it should be noted that human does not walk according to a predefined gait. Human style is performed using some aims and limitations like consuming the minimum energy, maintaining the balance during walking or crossing over obstacles, and being adaptive to the environment and circumstances. Based on these facts about human's walking, new visions about the control of the biped robot movements can be developed. The MPC technique that is on the basis of minimization of a cost function under several limitations looks to be very appropriate for controlling the bipeds. The MPC is a common control scheme planned for solving a sequence of optimum control problems under several restrictions [2]. The NMPC includes two sections: a nonlinear model of the system and an optimizer, which needs a cost function and possibly some constraints. The block diagram corresponding to the control approach of the suggested technique is presented in Fig. 3. As it is shown in Fig. 3, first the predictive model forecast the angles and angular velocities in predictive horizon. Then, based on predicted signals, the optimization part calculates the optimal input controls in control horizon in order to minimum the objective function. At the end, first value of the control input vector in control horizon is applied to robot and same loop is repeated again.

Several studies have utilized the MPC just for minimization of the energy. However, in this manuscript, moving the robot's COM forward and providing more appropriate supporting polygon are also taken into account in addition to the minimization of the energy consumption.

A common problem in the previous studies of robot's walking is that the gait length is predefined and constant. In a full stepping cycle, the biped has to initiate stepping in a stand up position. It must reach a steady limit cycle following several steps, which means nearly a fixed body development rate and fixed gait length. [5]. However, in situations, where the biped has to avoid large obstacles with unknown length and height, the gait length cannot be constant. Moreover, fixed gait length can result in more energy consumption. In addition, the robot may become unstable when external disturbances occur in these case. On the other hand, when using the NMPC, it is possible to alter the gait length to

overcome the aforementioned shortcomings. Moreover, the robot will walk more naturally like a human. The gait length is generated by defining some constraints in the optimal problem of the NMPC. Hence, in the suggested technique, the gait length of gait is not constant and the robot can stand at any appropriate point (e.g. prior to the obstacle or when external disturbances are incurred).

As it was stated before, the NMPC includes two phases: 1) the cost function and 2) the constraints. These two parts must be considered separately for the DSP and the SSP because these phases have different natures.

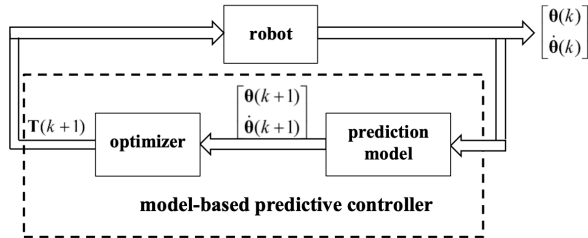


Fig. 3. Block diagram of control strategy of proposed method

3.1. Double Support Phase

The objective function and the constraints for the DSP stage are described below.

3.1.1. DSP Cost Function

There are two key goals that are considered in the cost function in this manuscript: 1) minimization of the energy and 2) constant velocity of the robot's COM

$$J^{DSP} = w_1 \sum_{i=0}^{N_c-1} \mathbf{T}(t+i\Delta t)^T \mathbf{T}(t+i\Delta t) + w_2 \sum_{i=1}^{N_p} [\dot{x}_{COM}(t+j\Delta t) - \alpha \dot{x}_{COM}^{desired}]^2 \quad (4)$$

where

$$\alpha = 1 - \frac{2}{1 + \exp\left(\frac{x_{COM}^{final} - x_{COM}(t+j\Delta t)}{\sigma}\right)} \quad (5)$$

and $\dot{x}_{COM}^{desired}$ and x_{COM}^{final} are the preferred horizontal velocity of the COM and location of the last stop point exactly prior the obstacle, respectively, and σ refers to a factor that controls the acceleration of the robot movement. At the start of movement, the error $x_{COM}^{final} - x_{COM}$ is very large and the value of α is almost one. When the robot is close to the goal or near the obstacle, the error and hence, α become zero. N_p is the prediction horizon and N_c is the control horizon. Δt introduces the sampling time, and w_1 and w_2 are the weighting coefficients, respectively.

3.1.2. DSP Constraints

The following constraints need to be defined for this phase:

1. The joint limitations for the robot that shows in Fig. 1 are

$$q_{i,min} \leq q_i \leq q_{i,max} \quad (6)$$

$$q_1 = \theta_1; \quad q_2 = \theta_1 - \theta_2; \quad q_3 = \theta_2 - \theta_3; \quad q_4 = \theta_3 + \theta_4; \quad q_5 = \theta_4 - \theta_5 \quad (7)$$

The controller must provide $q_2 \neq \pi$ and $q_5 \neq \pi$ to avoid singularities in the Jacobian matrix.

2. The actuator torques are limited to

$$T_{i,min} \leq T_i \leq T_{i,max} \quad (8)$$

3. The robot must maintain the erected posture during its walking

$$h_{min} \leq h_{hip} \leq h_{max} \quad (9)$$

where h_{hip} refers to the standard height of the robot's hip.

4. The torso has nearly 50% of robot's weight and plays the main role in the dynamic stability. The torso must be almost upright. Hence,

$$\theta_{min} \leq \theta_{trunk} \leq \theta_{max} \quad (10)$$

5. The robot must only move forward. Therefore, the velocity of the robot's COM in the x-direction must be positive

$$\dot{x}_{COM} \geq 0 \quad (11)$$

6. The swinging leg tip height should be above the land

$$y_e = 0 \quad (12)$$

7. As observed in Fig. 4, the supporting area for dynamic stability is

$$x_e \leq x_{ZMP} \leq x_b + \text{footlength} \quad (13)$$

8. For walking over the obstacles, the horizontal position of the knee should not collide with the barrier

$$x_{knee} \leq x_{O_2} + 0.02 \quad (14)$$

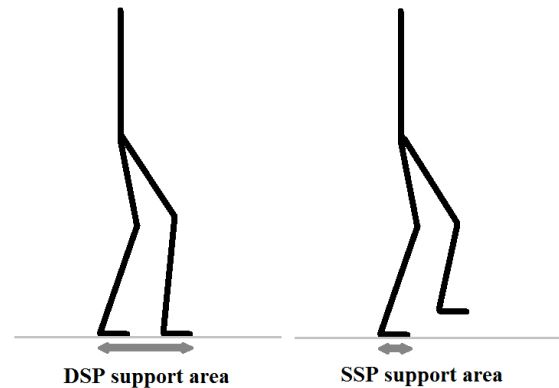


Fig. 4. Support area for DSP and SSP

where x_{O_2} is the x-coordinate of O_2 point (Fig. 2) and 0.02 m is added for safety distance.

3.2. Single Support Phase

The objective function and the constraints for the SSP phase are described in the followings.

3.2.1. SSP Cost Function

The first two goals in the cost function of the SSP are the same as in the DSP. An extra term should be added in this phase that makes the swing foot to decrease its height when the ZMP reaches its margin. This term can change the gait length when the robot is becoming unstable; e.g., when external disturbances like a sudden push is exerted on the robot. Hence, the cost function for the SSP can be expressed as

$$J^{SSP} = w_1 \sum_{i=0}^{N_s-1} \mathbf{T}(t+i\Delta t)^T \mathbf{T}(t+i\Delta t) + w_2 \sum_{i=1}^{N_p} [\dot{x}_{COM}(t+i\Delta t) - \alpha \dot{x}_{COM}^{desired}]^2 + \sum_{k=1}^{N_p} w_3(k) y_e(t+k\Delta t) \quad (15)$$

where y_e is the tip height (i.e. the y -coordinate) of the swing leg and w_3 is

$$w_3(k) = \begin{cases} 0 & \text{if } x_e(t+k\Delta t) \leq x_b \\ \eta \exp\left(\frac{\text{footlength} + \varepsilon}{\text{footlength} + x_b - x_{ZMP}(k) + \varepsilon} - 1\right) & \text{if } x_e(t+k\Delta t) > x_b \end{cases} \quad (16)$$

where x_e and x_b are the x -coordinate of the tip of the swinging and fixed legs, respectively, and ε is a small positive constant that prevents w_3 to become infinite. When the ZMP reaches its maximum acceptable position, which is equal to $(\text{footlength} + x_b)$, w_3 increases exponentially and magnifies the corresponding term in the cost function.

3.2.2. SSP Constraints

For smooth and standard stepping at slick surface, the following limitations are considered for the SSP phase:

1. The first five limitations are as same as the DSP limitations.
2. Dynamic stability should be assured with restriction of the ZMP in the support are

$$x_b \leq x_{ZMP} \leq x_b + \text{FootLength} \quad (17)$$

3. The tip height of the swinging leg must be in the following interval

$$0 \leq y_e \leq H_{\max} \quad (18)$$

4. The horizontal velocity of the tip must be adjusted to the robot's COM velocity

$$\begin{cases} \dot{x}_e \geq \beta_{\min} \dot{x}_{COM} \sin\left(\frac{\pi y_e}{2H_{\max}}\right) \\ \dot{x}_e \leq \beta_{\max} \dot{x}_{COM} \sin\left(\frac{\pi y_e}{2H_{\max}}\right) \end{cases} \quad (19)$$

5. During taking off, the vertical velocity of the tip should be positive and over landing it is needed to be negative and adjusted to the robot's COM velocity

$$\delta \dot{x}_{COM} \sin\left(\pi \frac{|x_e - x_b|}{H_{\max}}\right) \sin\left(\frac{\pi y_e}{H_{\max}}\right) + \text{sgn}(x_e - x_b) \dot{y}_e \leq 0 \quad (20)$$

For crossing over the barriers, the next constraints are needed to be investigated or replaced.

6. The tip height of the swinging leg must be limited to

$$\begin{cases} x_e \leq x_{O_2}, x_e \geq x_{O_3} \Rightarrow 0 \leq y_e \leq H_{O,\max} \\ x_{O_2} \leq x_e \leq x_{O_3} \Rightarrow H_{O,\min} \leq y_e \leq H_{O,\max} \end{cases} \quad (21)$$

where O_2 and O_3 are obstacle coordinates represented in Fig. 2.

7. The horizontal velocity of the tip is needed to be adjusted to the robot's COM velocity

$$\begin{cases} \dot{x}_e \geq \beta_{\min} \dot{x}_{COM} \sin\left(\frac{\pi x_e}{x_{O_2} + x_{O_3}}\right) \\ \dot{x}_e \leq \beta_{\max} \dot{x}_{COM} \sin\left(\frac{\pi x_e}{x_{O_2} + x_{O_3}}\right) \end{cases} \quad (22)$$

8. The vertical speed of the tip must be

$$\begin{cases} x_e < x_{O_2} \Rightarrow \dot{y}_e > 0 \\ x_{O_2} \leq x_e \leq x_{O_3} \Rightarrow \dot{y}_e = 0 \\ x_e > x_{O_3} \Rightarrow \dot{y}_e < 0 \end{cases} \quad (23)$$

9. The horizontal location of the knee must not impact with the barrier

$$x_{knee} \leq x_{O_2} + 0.02 \quad (24)$$

First, the biped robot walks on a flat ground naturally. If a barrier is sensed in the neighborhood of the robot, the controller controls the gait length (i.e., makes the gait length either shorter or longer) for stopping at a suitable distance before the barrier. If the biped robot can pass through the barrier, the controller does its task; if not, the robot stops. Since the biped robot in this manuscript is able to only move in the sagittal plane, it cannot go around the barrier.

3.3. Single Support Phase Impact

This phase is a transient phase that does not need any cost function. It is just necessary that the impact becomes as small as possible such that, the velocity of the swinging leg converges to zero during touching the ground.

4. Modeling with Neural Networks

Usually, the dynamic model of a biped robot contains some uncertainties. Moreover, the mass and inertia of all links may vary during time. Hence, a precise model is not always accessible. The proposed controller in this manuscript (NMPC) needs the robot dynamic model to forecast the robot future behavior. The Multi-Layers Perceptron (MLP) NNs are used in current research for overcoming the dynamic uncertainty of the robot. It is popular that NNs can estimate any nonlinear dynamic such as biped robots, with required accuracy. The general scheme of the NMPC with employing of neural networks as model identifiers is represented in Fig. 5. In this paper, for predicting future behavior of robot, neural network is utilized to overcome uncertainties and variation in robot dynamics model and its parameters. As it is shown in Fig. 5, first the MLP neural network predict the angles and angular velocities in predictive horizon. Then, the optimization block obtains the optimal torques in control horizon.

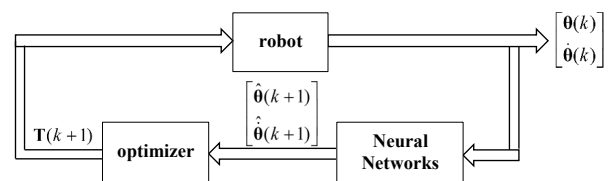


Fig. 5. General scheme of closed-loop system using NMPC with neural networks as model identifiers.

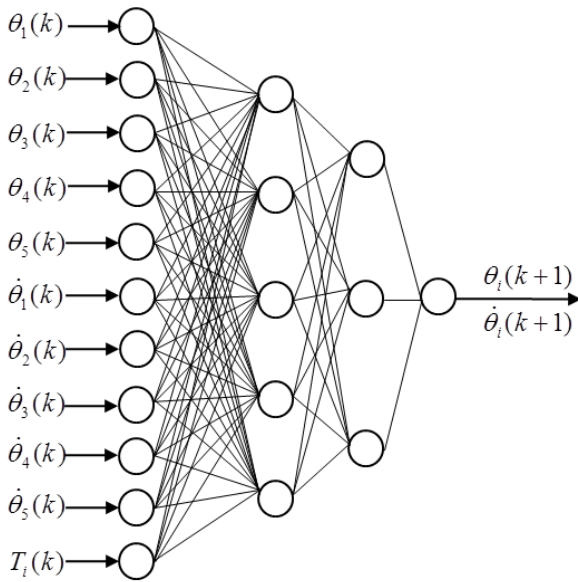


Fig. 6. Multilayers perceptron neural network structure

As it is depicted in Fig. 6, the inputs to the NNs are the angular position and velocity of all five joints and the torque of the corresponding joint, all at the current sampling time. The output is the predicted angular position or velocity of the corresponding joint at the next sampling time. Hence, there are twice as many NNs as the DOF of the robot; i.e., ten NNs are needed. The predicted quantities are fed back to the NNs over the prediction horizon (N_p). Then, these predicted values along with the cost functions and constraints (described in Section 3) are provided to the optimizer to compute the required torque for the corresponding joints of the robot over the control horizon (N_c). The first element of the predicted control laws is applied to the robot and the rest are discarded. The similar process is repeated during the next sampling time [40, 41].

The neural networks are trained off-line utilizing data collected from the robot walking and crossing over barriers. Levenberg-Marquardt algorithm is utilized for training of the network. As it is drawn in Fig. 6, two hidden layers with five and three neurons, respectively, are utilized for all NNs. The transfer functions of the hidden and output layers are of the hyperbolic tangent and linear types, respectively [42].

5. Stability Analysis

The stability analysis is one of the main and difficult concept in the area of biped robots. During walking, only one of the legs is on the ground that can make it unstable.

The biped robots do not meet the Lipschitz condition mainly because of the fact that their motion is periodic. The Poincaré return map is used to analyze periodic systems; hence, it is appropriate for the stability investigation of the biped robots [28]. The advantage of this method is that the Poincaré map reduces the study of the periodic orbits to the study of equilibrium points (or fixed points). However, the main problem in the Poincaré technique is to discover the Poincaré map that is very nonlinear and complicated and for a typical nonlinear system it is nearly not possible to perform that in a closed form because it requires the solution of a nonlinear differential equation. Numerical methods can be applied to calculate the return map, determine its constant points and predict eigenvalues for determination of the stability. However, the numerical calculations are typically

time intensive and doing them iteratively as part of a system design procedure can be cumbersome.

A more important thing is that numerical computations are not insightful in the sense that it is often difficult to provide a direct relation between the factors, that a designer can change in a system and existence or stability properties of fixed point of the Poincaré map [28, 34, 44]. Hence, an estimation of the Poincaré map can be performed by numerical calculations. However, these methods require long time to solve. The linearization of the Poincaré map around the constant point is one of the approaches utilized to solve this problem. This matrix is called the Jacobian matrix. After determining the Jacobian matrix, the eigenvalues of this matrix are calculated. If the absolute value of these eigenvalues are less than one, the robot stability is guaranteed.

5.1. Systems with Impulse Effect

Systems with impulse effects are used to model the inherently hybrid nature of the walking and running biped robots [28, 33]. Systems with impulse effects have a continuous phase described by differential equations and a discrete phase described by an instantaneous state reset event. A general periodic control system with impulse effect has the following form:

$$\Sigma: \begin{cases} \dot{\mathbf{x}} = \mathbf{f}(\mathbf{x}) + \mathbf{g}(\mathbf{x})\mathbf{u} & \mathbf{x}^- \notin S \\ \mathbf{x}^+ = \Delta(\mathbf{x}^-) & \mathbf{x}^- \in S \end{cases} \quad (25)$$

where \mathbf{x} , \mathbf{x}^- and \mathbf{x}^+ refer to the left and right limits of the system solution, \mathbf{u} represents the control input and S is the impact (or switching) surface, represented as

$$S = \{ \mathbf{x} \in \mathcal{X} \mid H(\mathbf{x}) = 0, H_0(\mathbf{x}) > 0 \} \quad (26)$$

where $H: \forall \mathbf{x} \in S, S \neq \emptyset$ and $\frac{\partial H}{\partial \mathbf{x}}(\mathbf{x}) \neq 0$. The solution for a system with impulse impacts is denoted as $\varphi(t, t_0, \mathbf{x}_0)$ for $t > t_0$ and $\mathbf{x}_0 \in \mathcal{X}$.

The geometric interpretation for a Poincaré return map for a system with impulse impacts is demonstrated in Fig. 7. The Poincaré section is chosen as the switching surface S . A Poincaré map exists when $P(\mathbf{x}^-) = \mathbf{x}^-$ holds.

5.2. Biped Robot Dynamic as a system with Impulse effects

For stability analysis, the SSP and Impact dynamics are considered because the DSP phase is relatively more stable and does not comprise big challenges comparing with other two phases. The SSP dynamic were expressed in (1). The \mathbf{q} and $\dot{\mathbf{q}}$ vectors refer to the relative angular positions and velocities where $\mathbf{0} = \mathbf{M}\mathbf{q}$ (Fig.1). Equation (1) can be represented as

$$\mathbf{D}(\mathbf{q})\ddot{\mathbf{q}} + \mathbf{H}(\mathbf{q}, \dot{\mathbf{q}}) + \mathbf{G}(\mathbf{q}) = \mathbf{T}_q \quad (27)$$

Hence, the steady-state form of the SSP is

$$\dot{\mathbf{x}} = \begin{bmatrix} \dot{\mathbf{q}} \\ \mathbf{D}^{-1}(\mathbf{q})(-\mathbf{H}(\mathbf{q}, \dot{\mathbf{q}}) - \mathbf{G}(\mathbf{q})) \end{bmatrix} + \mathbf{D}^{-1}(\mathbf{q})\mathbf{T}_q \quad (28)$$

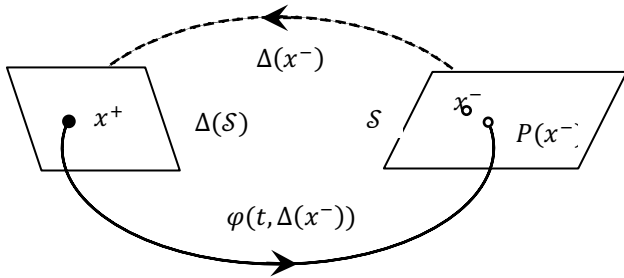


Fig. 7. The geometric expression of a Poincaré return map for a dynamic with impact

where $x = [q, \dot{q}]^T$. Using these new variables and based on (3), the impact equation is

$$\dot{q}^+ = \dot{q}^- + M^{-1}D^{-1}(q)J^T(q)[J(q)D^{-1}(q)J^T(q)]^{-1}(-J(q)M\dot{q}^-) \quad (29)$$

where M is

$$M = \begin{bmatrix} 1 & 0 & 0 & 0 & 0 \\ 1 & -1 & 0 & 0 & 0 \\ 1 & -1 & -1 & 0 & 0 \\ -1 & 1 & 1 & 1 & 0 \\ -1 & 1 & 1 & 1 & -1 \end{bmatrix} \quad (30)$$

Therefore based on (25), $x^+ = \Delta(x^-) = \begin{bmatrix} \Delta(q^-) \\ \Delta(\dot{q}^-, \dot{q}^-) \end{bmatrix} = \begin{bmatrix} 1 \\ \Delta(q^-, \dot{q}^-) \end{bmatrix}$ where $\Delta(q, \dot{q})$ is the right

hand side of (29), $\Delta(q^-)$ is equal to one as it is supposed that the impact only affects the angular velocities and not the joint angles. The switching surface occurs during the SSP impact time and it means that when the tip height of the swinging leg becomes zero. That is

$$S = \{x | y_{sw}(q) = 0, x_{sw}(q) > 0\} \quad (31)$$

where $[x_{sw}(q), y_{sw}(q)]^T$ is the coordinate of the tip of the swinging leg.

5.3. Fixed Point

In the sense of the Poincaré map, a periodic system is steady when it reaches a special point after some cycles with any initial condition. This point is named the “fixed point” since it is similar at the end of all cycles. As it was stated previously, the Poincaré map has a simple idea; however, its implementation to nonlinear and complicated system, like biped robots, is hindered by looking for a closed-form solution to the nonlinear dynamic equations governing the system. One method is linearization of the Poincaré map around the working point. For linearization of the Poincaré map, a constant point must be discovered first. If the trajectory was designed off-line, then it would be really easy to find the constant point as the state variables just prior to the impact phase in the reference route [32-34]. Though, in the suggested technique no predefined trajectory exists, mostly because of the advantages that were explained before. To define the constant point, the robot walks for a few steps with different primary conditions. This procedure is repeated 100 times. Since the primary condition is changed, a different constant point is achieved every time the robot walks. The constant point is computed as the average of 100 state variables just afore the impacts occur.

5.4. Jacobian Matrix

The Poincaré map $P(x)$ induces a discrete-time system $x^{k+1} = P(x^k)$. The linearization about a constant point determines the closed-loop system stability [33]. Let define $\delta x^k = x^k - x^*$. The Poincaré map linearized around the constant point $x^* = [q^*, \dot{q}^*]^T$ yields that following linear system:

$$\delta x^{k+1} = A \delta x^k \quad (32)$$

Because the biped has 5 links, q and \dot{q} are 5×1 vector and refers to a 10×1 vector. Hence, matrix A is a 10×10 square matrix that is called the Jacobian for the Poincaré map and is calculated as follows:

$$A = [A_1 \ A_2 \ \dots \ A_{10}]_{10 \times 10} \quad (33)$$

where

$$A_i = \frac{P(x^* + \Delta x_i) - P(x^* - \Delta x_i)}{2\Delta x_i}, \quad i = 1:10 \quad (34)$$

in which $\Delta x_i = \Delta q_i$ for $i = 1:5$ and $\Delta x_i = \Delta \dot{q}_i$ for $i = 6:10$; Δx_i are small perturbations demonstrated to compute the linearized dynamic. Hence, (34) should be explicated as the scalar perturbation utilized in calculating Δx_i . Generally, the computation of the Jacobian matrix depends on the amplitude of perturbation Δx_i . The computation of matrix requires 20 evaluations of function $P(x^* \pm \Delta x_i)$. The local exponential stability of a fixed point of the Poincaré map is achieved, if and only if the magnitude of the eigenvalues of are strictly less than one [43].

6. Simulation Results

The biped robot parameters are adopted from [26] (Table 1). This robot weights 49.5 kg and is 1.73 m tall. Table 2 displays the least and highest value of design parameters. Other factors are

$$\text{FootLength} = 15\text{cm}, \dot{x}_{\text{COM}}^{\text{desired}} = 1\text{m/s}, N_p = 5, N_c = 4, w_1 = 100, w_2 = 0.01, \sigma = 0.03, \Delta t = 0.02\text{s},$$

$$\text{Obstacle_Height} = 40\text{cm}, \text{Obstacle_Length} = 15\text{cm}.$$

Table 1. Biped robot parameters

Link No.	1	2	3	4	5
Length (m)	0.53	0.5	0.70	0.5	0.53
Mass (kg)	3.7	8.55	25	8.55	3.7
Inertia (kgm ²)	0.3	0.3	0.3	0.3	0.3
Location of center of mass (m)	0.285	0.31	0.4	0.31	0.285

Table 2. The value of design parameters

Variable	h_{hip}	θ_{trunk}	T_i (walking on flat surface)	T_i (stepping over obstacle)	H_o	β

Minimum	0.9 8 m	-3°	-200 Nm	-300 Nm	Obstacle_Hei ght + 0.01m	4
Maximum	1.0 8 m	3°	200 Nm	300 Nm	Obstacle_Hei ght + 0.03m	1 0

The *fmincon* function in the MATLAB optimization toolbox is utilized to solve the optimization problem devoted to minimizing a controlled nonlinear multivariable function. The *fmincon* is on the basis of the Sequential Quadratic Programming (SQP) algorithm. The SQP is an iterative method in which the objective is substituted with a quadratic estimate and the limitations by linear estimates.

The biped robot starts walking from a stand-up location and follows a desired development velocity. As the biped reaches the obstacle, it has to step a shorter or longer gait than its normal gait and stops before the obstacle and then walk over it. After that, the biped robot steps an almost half a cycle gait and starts normal walking until it detects a new obstacle or reaches the final destination, where it has to decrease its walking velocity until it comes to a full stop. Knowing the location of the base foot, the biped orientation can be defined with position of the hip and swing foot. The primary orientation of the biped is chosen near to the standing up orientation as

$$x_b = 0 \text{ m}, x_e = -0.25 \text{ m}, y_e = 0 \text{ m}, x_h = -0.12 \text{ m}, y_h = 0.88 \text{ m}$$

Three different cases are carried out to display the efficiency of the suggested control technique. In the first case, the robot walks and steps over a big obstacle without any uncertainty in the dynamic model. Fig. 8 represents several stepping cycles. It should be mentioned that the final cycle is shorter due to detecting the obstacle. The robot stops right before the obstacle and puts its feet next to each other. The ZMP in the *x*-direction steps forward and is in the supporting polygon always during the DSP and SSP, yielding dynamic stability to the robot (Fig. 9). The hip and the tip of the swing foot are represented in Fig. 10. The swing foot has nearly parabolic route and the height of the hip is limited. This means that the biped has a flat and standard walk. The last cycle, which is shorter, can be seen in this figure. Fig. 11 shows the required joints torque, which are within the saturation limits of ± 200 Nm. Three stages of walking over the obstacle are demonstrated in Fig. 12. To avoid any contact of the swinging leg with the obstacle, a 2 cm-wide safety clearance is considered around the obstacle (the green shade in Fig. 12). Fig. 13 indicates that the horizontal position of the ZMP is maintained in the supporting polygon during stepping over the obstacle, which means that the biped stability is achieved. Fig. 14 displays that the swing foot tip is raised to higher heights than the obstacle and next, it moves horizontally to pass the obstacle. Then, the biped lowers the swing foot tip until it lands. It is clear that the swing foot tip has no contact with the obstacle during the crossing over. In the SSP1 and DSP, the vertical position of the hip is raised to provide its easier stepping over the obstacle and then, it is lowered during the SSP2 and finally back to the normal position. Fig. 15 displays that the joints torque are inside the pre-defined boundaries (± 300 Nm).

In the second case of simulations, to display the robustness of the suggested NMPC using NNs as the predictive models, the mass and inertia of the torso links are increased by 20%. In Fig. 16 and 17, it is obvious that by using the dynamic equation of the robot as the prediction model and considering

these uncertainties in the parameters, the robot cannot walk, step over obstacle and keep its balance. However, as Fig. 18 shows, when NNs are employed as the model, position of the swing foot tip and position of the hip do not come in contact with the barrier. In this case, the NNs produce bigger joint torques with larger variations for maintaining the robot stability. Moreover, the joint torques are within the predefined boundaries.

In the third case, an immediate disturbing push is applied to the trunk joint of the robot at $t = 0.33$ sec. This disturbance is modeled as a 25 Nm impact torque during 0.1 sec (the impact time). As Fig. 19 shows, the horizontal position for the swing foot is clipped (i.e. the robot lowers its swing foot abruptly) when the external disturbance is exerted on the biped. This means that the gait length is reduced by the controller and the DSP happens sooner for establishing a wider supporting area to maintain the robot stability. In fact, in this case, the adaptive term (w_3) in the cost function is increased to higher values as compared to the other two terms for a short period of time to guarantee the biped stability. Fig. 20 displays a similar case but without this adaptive term in the cost function. As it can be seen in this figure, the biped cannot maintain its balance and falls.

To study the stability of the suggested control technique with the Poincaré return map, the phase-plane for five joints of the biped robot is achieved (Fig. 21). As this figure shows, after the transition behavior of all joints, the $q-\dot{q}$ curve converges to a periodic movement. The straight lines connect two cycles of motion related with the impact phase. It is clear that the periodic cycles are not similar because there is no predefined desired trajectory and the robot walks freely and naturally as a human.

The numerical values of the state variables for 100 repetition of walking just afore the impact occurs are presented in Fig. 22. The constant point (i.e. the average of these points) is

$$x^* = [q^*, \dot{q}^*]^T = \begin{bmatrix} 0.7213 & 1.1426 & -0.3774 & 0.7684 & 1.1137 \\ 0.5421 & -0.4182 & 0.9732 & -0.4737 & 0.4145 \end{bmatrix}$$

The perturbations Δx_i are equal to 0.004. The eigenvalues of the Jacobian matrix $A_{10 \times 10}$ are

$$\lambda_1 = -0.993, \lambda_2 = 0.714, \lambda_3 = 0.6044, \lambda_{4,5} = -0.0964 \pm 0.0881i$$

$$\lambda_{6,7} = -0.219 \pm 0.0924i, \lambda_8 = 0.1105, \lambda_9 = -0.029, \lambda_{10} = 0.0441$$

All eigenvalues have magnitude of less than one. Hence, the closed-loop system is stable based on the Poincaré stability criteria.

As it was mentioned before, are small perturbations introduced to compute the linearized model and the Jacobian matrix. Generally, computation of the Jacobian matrix is sensitive to the amplitude of perturbation Δx_i . Fig. 23 shows variation of number of stable eigenvalues based on the variation of Δx_i . As this figure shows, If Δx_i are selected in the range of [0.003, 0.005], then the Jacobian matrix stability is guaranteed. For smaller or larger Δx_i , there are less than 10 stable eigenvalues. This fact can be found from the amplitude of perturbations. As an example, when perturbations are small, then the denominators in (34) become very small. Consequently, the columns of A_i become very large, which produces large eigenvalues.

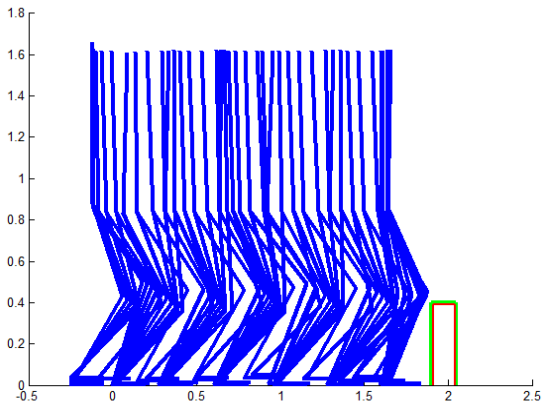


Fig. 8. Walking on flat ground and stopping right before barrier

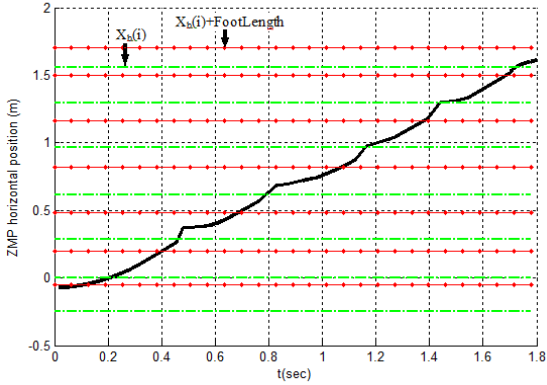


Fig. 9. ZMP horizontal position in walking on flat surface

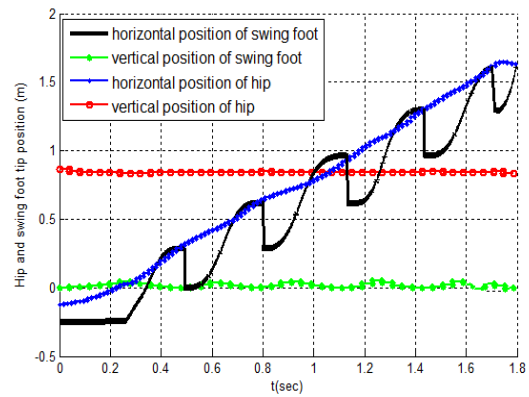


Fig. 10. Hip and tip of swing foot position for walking on flat ground right before obstacle

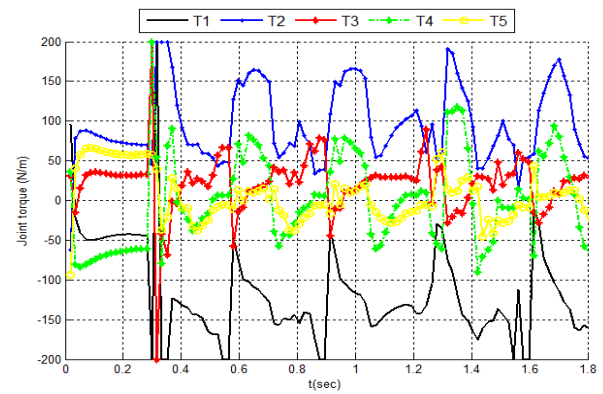


Fig. 11. Joints torque for walking on flat surface

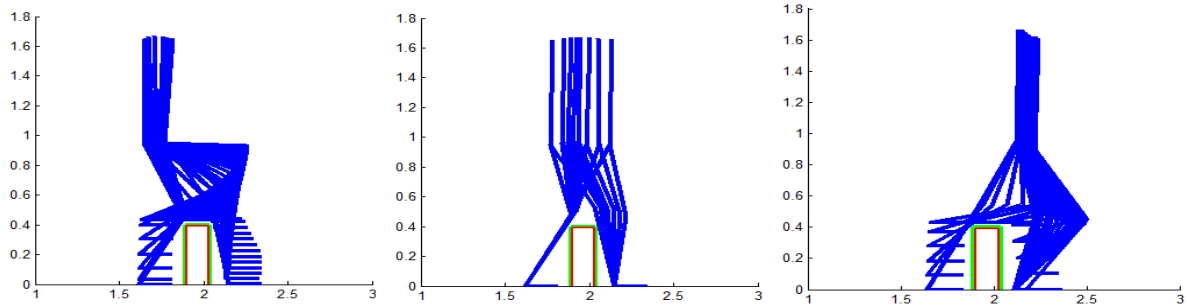


Fig. 12. crossing over obstacle

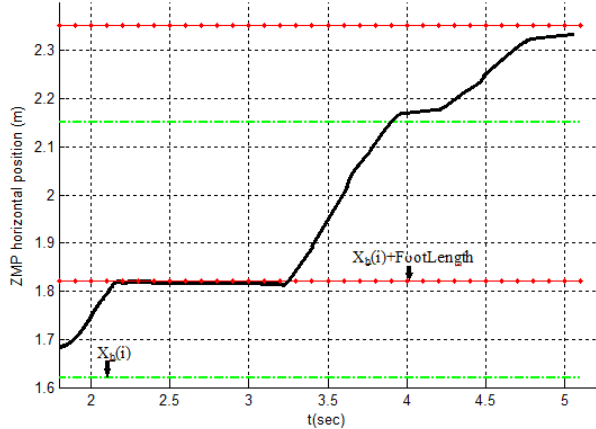


Fig. 13. ZMP horizontal position in crossing over barrier

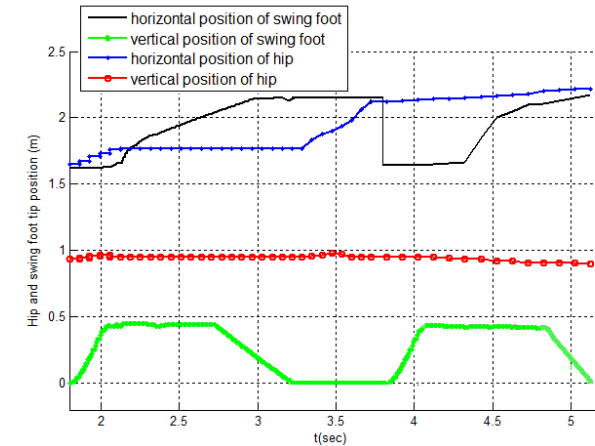


Fig. 14. Hip and tip of swing foot position in crossing over barrier

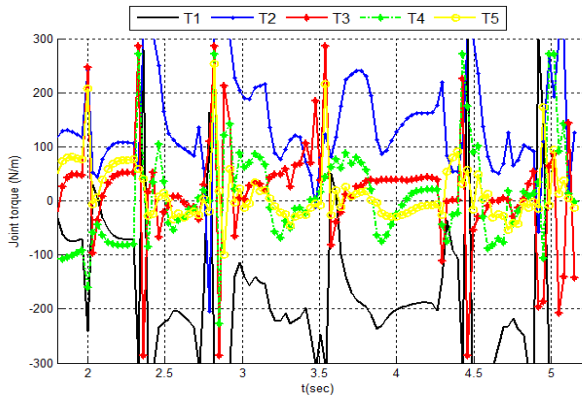


Fig. 15. Joints torque in stepping over obstacle

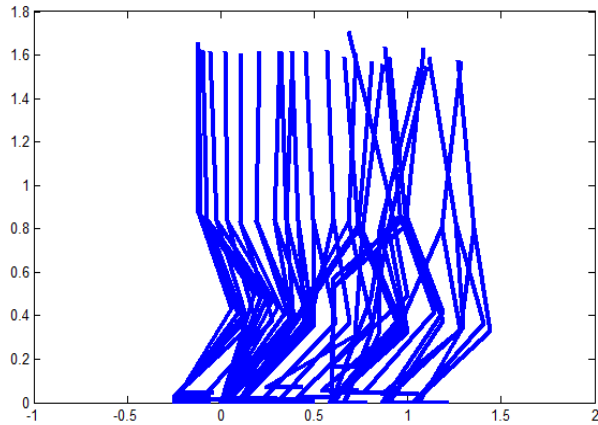


Fig. 16. Walking on flat ground and stopping right before barrier with existing 20% uncertainties in mas and inertia of torso link

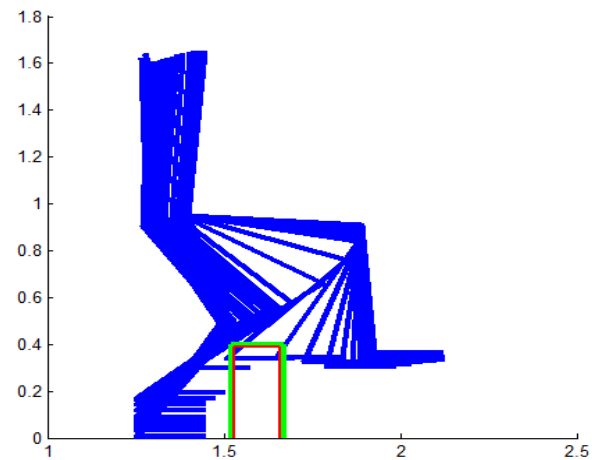


Fig. 17. Stepping over obstacle with existing 20% uncertainties in mas and inertia of torso link

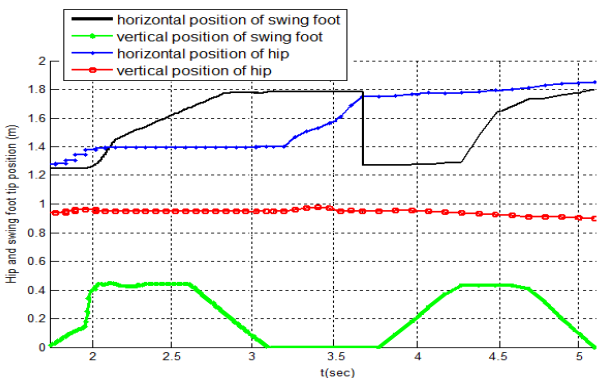


Fig. 18. Hip and tip of swing foot position in crossing over barrier and dynamic identification with neural network with existing 20% uncertainties in mas and inertia of torso link

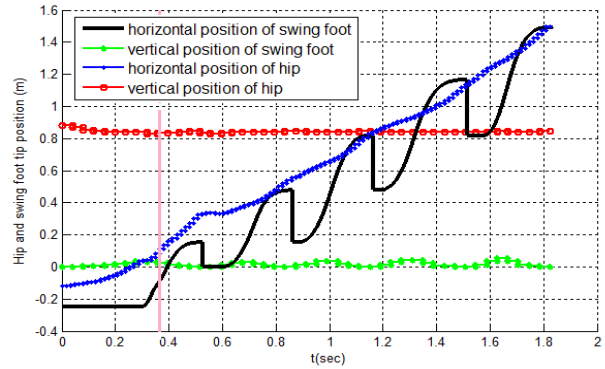


Fig. 19. Hip and tip of swing foot position in crossing over barrier and dynamic identification with neural network with existing 20% uncertainties in mas and inertia of torso link

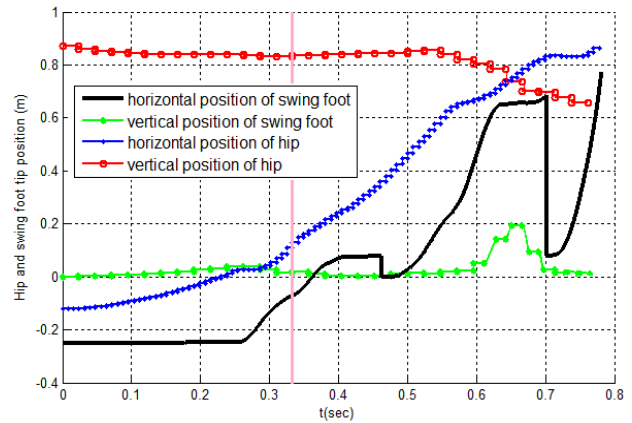
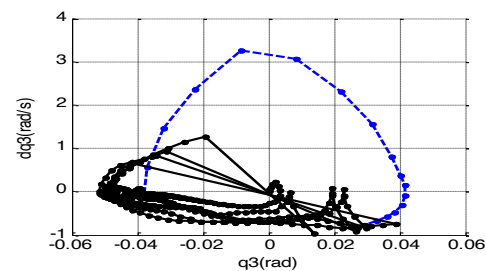
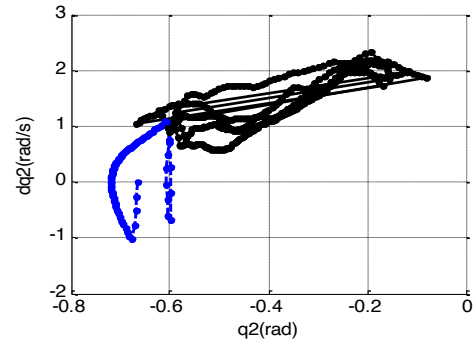
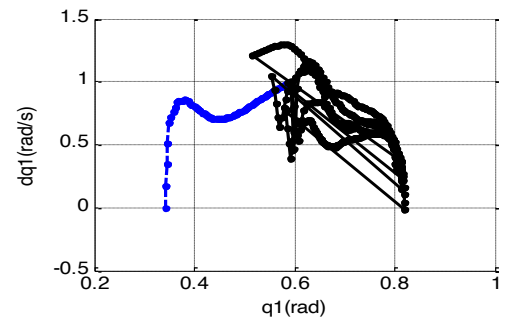


Fig. 20. Hip and tip of swing foot position in walking on flat surface while there is a sudden disturbing push without the adaptive term w_3 in the objective function



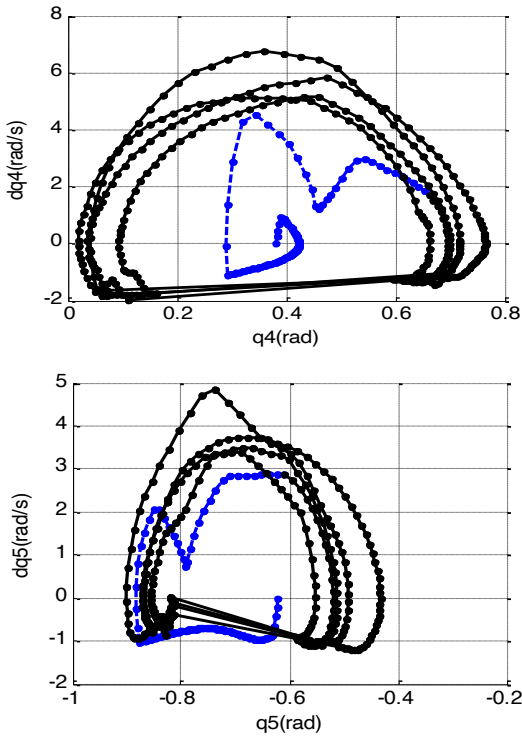


Fig. 21. Phase-plane for five joints of robot

In the case of stepping over obstacles, many papers considered very small obstacles that make them not

appropriate for comparison with proposed method in this manuscript. The humanoid robots like HRP-2 [18, 19] and Bonten-Maru II [22] have been shown good performance in stepping over obstacles. In [19], robot can cross over an obstacle with 15 cm height and 5 cm width. Also, in simulation results, it is indicated that this robot can step over 25 cm height obstacle but there is not any safe area around the target. Even considering a 25 cm height obstacle, HRP-2 can cross over an obstacle with 15% of its height but in the current research this ratio is 23% plus the safety clearance. Furthermore, in this manuscript, the obstacle width is much larger (15cm). In [19], ZMP is considered to guarantee the stability problem. A predefined trajectory is designed for the tip of the swinging leg that can be adapted during stepping over the obstacle. Hence, different trajectories should be designed for crossing over different obstacles. However, using the proposed method just the size of the obstacle suffices to make a successful walk. In [19], the ZMP and waist position of HRP-2 in directions X and Y , including horizontal and vertical foot situations for walking over a 15 cm height and 5 cm width plus 3 cm safety boundary. As it is presented, the robot can cross over obstacle and keep its balance but control technique is steel based on a predefined trajectory that reduces freedom process of the robot when facing unknown conditions. On the other hand, in this paper, there is no off-line trajectory and the robot can find an optimal way to step over barriers and keep its balance even when there are unforeseen situations.

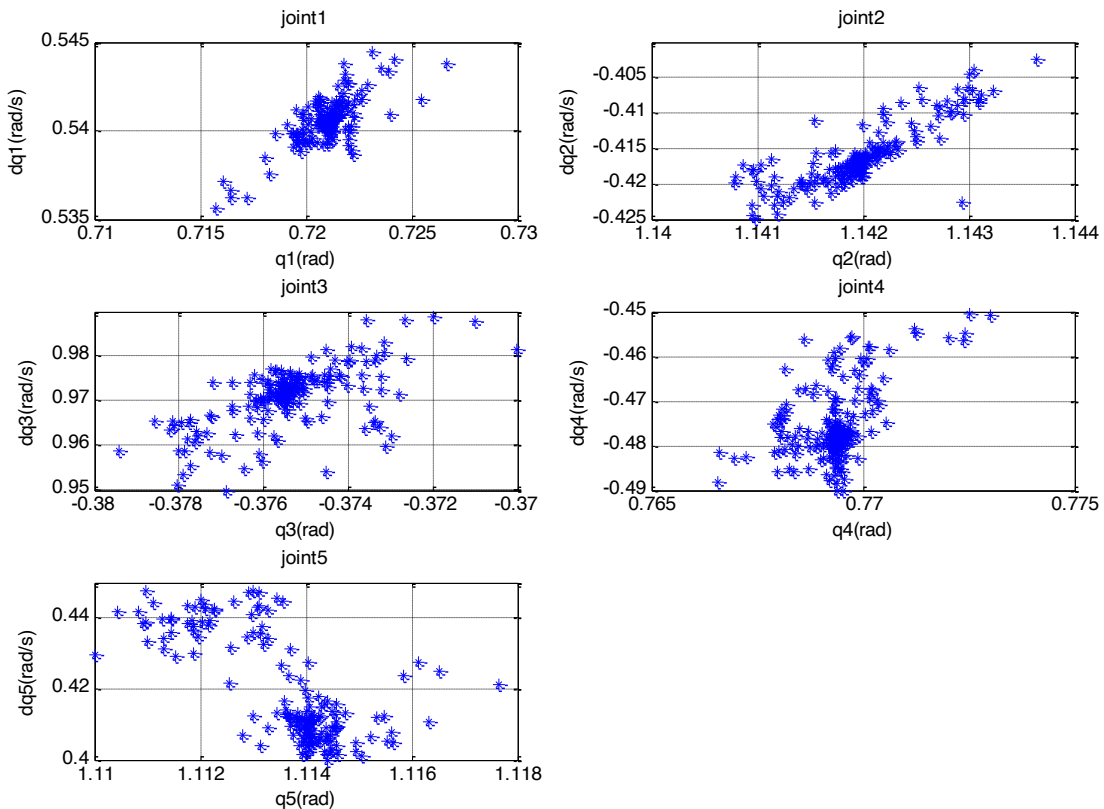


Fig. 22. The states of robot right before impact with small perturbation in initial conditions

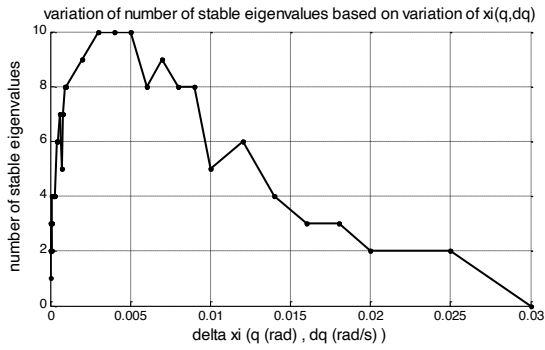


Fig. 23. Variation of number of stable eigenvalues based on variation of stable eigenvalues.

6. Discussion

Biped robots must move in the environment where humans live. Therefore, they must have the ability to move on all kinds of surfaces and cross different obstacles and go up and down stairs. Due to the possibility of more instability in such movements, the complexity of the control problem is determined. Generally, in the related papers that have worked on obstacle crossing for biped robots, very small obstacles have been considered. But the HRP-2 humanoid robot has shown a good ability to cross relatively high obstacles [19]. The obstacle that the robot crosses has a height of 15 cm and a width of 5 cm. It has been shown in the simulations that this robot can pass an obstacle with a height of 25 cm, but in this case there is no safety distance. Despite this obstacle, the ratio of the height of the robot (1.65 m) to the height of the obstacle is 15%, which in the proposed paper is 23% with despite the 3 cm security area. Also, the width of the barrier in [19] is only 5 cm, which in the proposed paper is 3 times (15 cm).

In [19], preview control is used to generate an online trajectory for the tip of the swinging leg and waist. They made the robot's movement dynamic and used the ZMP criterion to ensure stability. The authors reduced the speed of the robot's

ankle when it hit the ground, so that the amount of impact on the ankle was reduced as much as possible. In order to ensure that the foot does not hit the obstacle, an area around the obstacle is considered where the robot can reach the border of this area at most. In fact, the robot sees the obstacle as larger than its actual size. Figures 24 and 25 show this area and how the robot's foot passes over it. For comparison, in the proposed paper, the movement trajectory of the swinging toe has the ability to adapt. In [19], For the robot to cross the obstacle, a reference trajectory for the moving toe and waist is generated according to the dynamic stability and zero moment point of the robot. This trajectory has the ability to adapt to obstacle conditions. Fig. 26 shows the trajectory generated for the moving tip and Figures 27 and 28 show the reference trajectory of the zero moment point and the position of the moving tip of the robot's leg and hip in [19]. Therefore, in order to pass different obstacles, different trajectories must be produced for the tip of the swinging leg, while in the proposed paper, the robot generates its movement trajectory in an online way by only understanding the height and width of the obstacle and the determined restrictions. Although HRP-2 has passed the obstacle successfully and at a suitable speed, its control method is still based on the predetermined reference trajectory. In the event that the predictive control method presented in the proposed paper does not use any predefined desired trajectory and the movement trajectory is generated in an optimal and online manner and is provided to the robot, this is one of the most important reasons for the superiority of the proposed method in this paper.

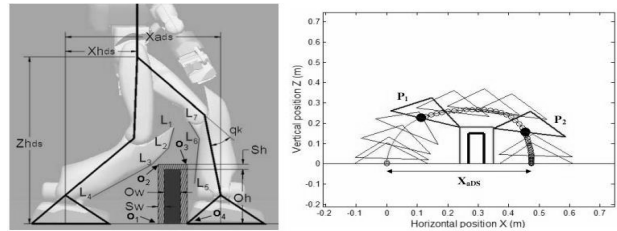


Fig. 24. Safety zone around the obstacle to prevent collision in [19]



Fig. 25. Crossing over obstacle of HRP-2 in [19]

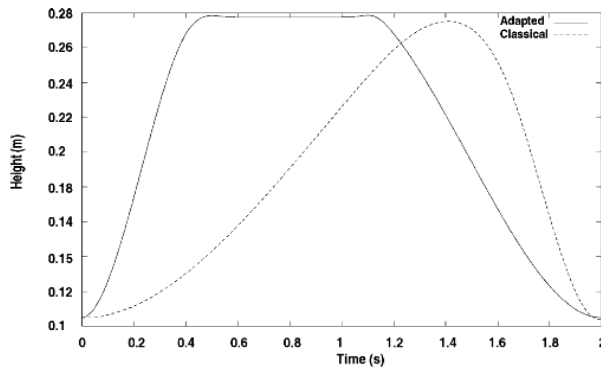


Fig. 26. Desired trajectory for the tip of the swinging leg in [19]

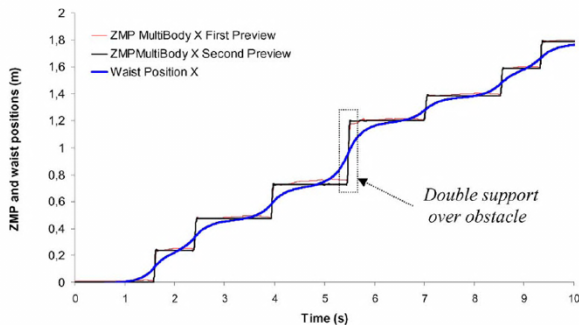


Fig. 27. ZMP and waist positions in [19]

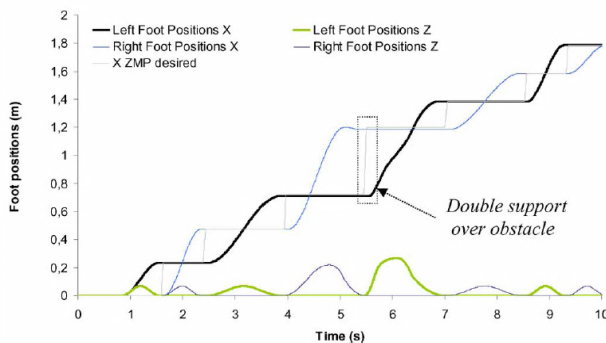


Fig. 28. Left and right foot position and the desired ZMP in [19]

7. Conclusion

This manuscript suggested a control technique for passing and crossing over large barriers and obstacles for biped robots. The NMPC is applied to control the robot with no off-line path planning. Due to the benefits of the NMPC, stepping and passing over obstacles is matched to human walking patterns. Another benefit of the presented method is that the gait length is not constant and the NMPC identifies it by calculating an optimization problem on the basis of different situations, stopping before any obstacle or a special position, dynamic stability of the robot, and external disturbances, which are defined as constraints of the optimization problem. In contrast to other approaches reported in the related literature, the robot can cross over a rather large barrier while keeping its balance. Since the NMPC is a model-based technique, NNs have been applied for identifying the dynamic of robot as well as handling uncertainties in the parameters of robot. The biped robot that is utilized in this manuscript weighs 49.5 kg weight and is 1.73 m tall; it could step over a 40×15 cm obstacle (40% of the robot's leg length) in the sagittal plane with maximum velocity of 1 m/s. Moreover, the suggested control technique was capable of rejecting external disturbances such as sudden pushes. The stability test of the suggested technique was studied using the Poincaré return map. For linearization of the Poincaré map, fixed point was needed. Since there was no predefined route, the constant point was computed on the basis of the mean of different cycle of walking with various initial conditions. Inspecting the eigenvalues of the Jacobian matrix indicated that the closed-loop system is stable. Simulation outcomes also indicated success of the proposed control method.

This is an Open Access article distributed under the terms of the Creative Commons Attribution License.



References

- Grizzle, J. W., Chevallereau, C., Sinnet, R. W., Ames, A. D., "Models, feedback control, and open problems of 3D bipedal robotic walking". *Automatica*, 50(8), 2014, pp. 1955-1988.
- Azevedo, C., Poignet, P., Espiau, B., "Online optimal control for biped robots". *IFAC Proceedings Volumes*, 35(1), 2002, pp. 199-204.
- Wieber, P. B., "Trajectory free linear model predictive control for stable walking in the presence of strong perturbations". *IEEE-RSJ International Conference on Humanoid Robots*, Genova, Italy: IEEE, 2006, pp. 137-142.
- Diedam, H., Dimitrov, D., Wieber, P. B., Mombaur, K., Diehl, M., "Online walking gait generation with adaptive foot positioning through linear model predictive control". *IEEE-RSJ International Conference on Intelligent Robots and Systems*, Nice, France: IEEE, 2008, pp. 1121-1126.
- Parsa, M., Farrokhi, M., "Robust nonlinear model predictive trajectory free control of biped robots based on nonlinear disturbance observer". *Iranian Conference on Electrical Engineering*, Isfahan, Iran: IEEE, 2010, pp. 617-622.
- Ibanez, A., Bidaud, P., Padois, V., "A distributed model predictive control approach for robust postural stability of a humanoid robot". *IEEE International Conference Robotics and Automation*, Hong Kong, China: IEEE, 2014, pp. 202-209.
- Wittmann, R., Hildebrandt, A. C., Wahrmann, D., Rixen, D., Buschmann, T., "Real-time nonlinear model predictive footstep optimization for biped robots". *IEEE-RAS International Conference on Humanoid Robots*, Seoul, Korea (South): IEEE, 2015, pp. 711-717.
- Luo, R. C., Chen, C. C., "Biped walking trajectory generation based on three-mass with angular momentum model using model predictive control". *IEEE Transactions on Industrial Electronics*, 63(1), 2016, pp. 268-276.
- Janardhan, V., Prasanth Kumar, R., "Generating feasible solutions for dynamically crossing a wide ditch by a biped robot". *Journal of Intelligent and Robotic Systems*, 88, 2017, pp. 37-56.
- Janardhan, V., Prasanth Kumar, R., "Online trajectory generation for wide ditch crossing of biped robots using control constraints". *Robotics and Autonomous Systems*, 97, 2017, pp. 61-82.
- Deng, K., Zhao, M., Xu, W., "Bifurcation gait suppression of a bipedal walking robot with a torso based on model predictive control". *Robotics and Autonomous Systems*, 89, 2017, pp. 27-39.
- Joe, H. M., Oh, J. H., "Balance recovery through model predictive control based on capture point dynamics for biped walking robot". *Robotics and Autonomous Systems*, 105, 2018, pp. 1-10.
- Zamparelli, A., Scianca, N., Lanari, L., Orioli, G., "Humanoid gait generation on uneven ground using intrinsically stable MPC". *IFAC-PapersOnLine*, 51, 2018, pp. 393-398.

14. Villa, N. A., Wieber, P. B., "Model predictive control of biped walking with bounded uncertainties". *International Conference on Humanoid Robotics (Humanoids)*, Birmingham, UK: IEEE, 2017, pp. 836-841.
15. Yu, Z., Zhou, Q., Chen, X., Li, Q., Meng, L., Zhang, W., Huang, Q., "Disturbance rejection for biped walking using zero-moment point variation based on body on acceleration". *IEEE Transactions on Industrial Informatics*, 15(4), 2019, pp. 2265-2276.
16. Martinez-Foseca, N., Castaneda, L. A., Uranga, A., Luviano-Juarez, A., Chairez, I., "Robust disturbance rejection control of a biped robotic system using high-order extended state observer". *ISA Transactions*, 62, 2016, pp. 276-286.
17. Guan, Y., Sian, N. E., Yokoi, K., "Motion planning for humanoid robots stepping over obstacles". *IEEE-RSJ International Conference on Intelligent on Robots and Systems*, Edmonton, AB, Canada: IEEE, 2005, pp. 363-369.
18. Guan, Y., Sian, N. E., Yokoi, K., "Stepping over obstacles with humanoids robots". *IEEE Transactions on Robotics*, 22(5), 2006, pp. 958-973.
19. Stasse, O., Verrelst, B., Vanderborcht, A. H. B., Yokoi, K., "Strategies for humanoid robots to dynamically walk over large obstacles". *IEEE Transactions on Robotics*, 25(4), 2009, pp. 960-967.
20. Hwang, C. L., Wu, H. C., Lin, M. L., "The stepping over an obstacle for the humanoid robot with the consideration of dynamic balance". *Proceeding of SICE Annual Conference*, Taipei, Taiwan: IEEE, 2010, pp. 2260-2268.
21. Akhtaruzzaman, M., Shafie, A. A., "Joint behaviors of a humanoid platform while overcoming an obstacle". *Advances Applied Science Research*, 2, 2011, pp. 299-311.
22. Yussof, H., "Biped locomotion of a 21-DOF humanoid robot for application in real environment". *Procedia Engineering*, 41, 2012, pp. 1566-1572.
23. Wahrmann, D., Wu, Y., Sygulla, F., Hildebrandt, A-C., Wittmann, R., Seiwald, P., Rixen, D., "Time-variable, event-based walking control for biped robots". *International Journal of Advanced Robotic Systems*, 15, 2018, pp. 1-9.
24. Delfin, J., Becerra, H. M., Arechavaleta, G., "Humanoid navigation using a visual memory with obstacle avoidance". *Robotics and Autonomous Systems*, 109, 2018, pp. 109-124.
25. Sabourin, C., Bruneau, O., "Robustness of the dynamic walk of a biped robot subjected to disturbing external forces by using CMAC neural networks". *International Journal of Robotics and Autonomous Systems*, 51(2-3), 2005, pp. 81-99.
26. Wang, X., "Balance Control for a Standing Biped and Stability Analysis Using the Concept of Lyapunov Exponent". Doctoral Dissertation of University of Manitoba, Canada, 2008, pp. 1-154.
27. Gil, C. R., Calvo, H., Sossa, H., "Learning an efficient gait cycle of a biped robot based on reinforcement learning and artificial neural networks". *Journal of Applied Science*, 9, 2019, pp. 1-24.
28. Grizzle, J. W., Abba, G., Plestan, F., "Asymptotically stable walking for biped robots: analysis via systems with impulse effects". *IEEE Transaction on Automatic Control*, 46, 2001, pp. 51-64.
29. Westervelt, E. R., Grizzle, J. W., Koditschek, D. E., "Hybrid zero dynamics of planar biped walkers". *IEEE Transaction on Automatic Control*, 48, 2003, pp. 42-56.
30. Aoi, S., Tsuchiya, K., "Stability analysis of a simple walking model driven by an oscillator with a phase reset using sensory feedback". *IEEE Transaction on Robotics*, 22, 2006, pp. 391-397.
31. Znegui, W., Gritli, H., Belghith, S., "Design of an explicit expression of the Poincare map for the passive dynamic walking of the compass-gait biped model". *Chaos, Solitons and Fractals*, 130, 2020, pp. 109436.
32. Morris, B. J., "Stabilizing Highly Dynamic Locomotion in Planer Bipedal Robots with Dimension Reduction Control". Doctoral Dissertation of University of Michigan, USA, 2008, pp. 1-98.
33. Chevallereau, C., Grizzle, J. W., "Asymptotically stable walking of a five-link under actuated 3-D bipedal robot". *IEEE Transactions on Robotics*, 25, 2009, pp. 37-50.
34. Luo, J., Wang, S., Zhao, Y., Fu, Y., "Variable stiffness control of series elastic actuated biped locomotion". *Intelligent Service Robotics*, 11, 2018, pp. 225-235.
35. Kumar Mandava, R., Katla, M., Vundavili, P. R., "Application of hybrid fast marching method to determine the real-time path for the biped robot". *Intelligent Service Robotics*, 12, 2018, pp. 125-136.
36. Kolathaya, S., "Local stability of PD controlled bipedal walking robots". *Automatica*, 114, 2020, 108841.
37. Kalamian, N., Farrokhi, M., "Dynamic walking of biped robots with obstacles using predictive controller". *International Conference on Computer Knowledge Engineering*, Mashhad, Iran: IEEE, 2011, pp. 160-165.
38. Kalamian, N., Farrokhi, M., "Stepping of biped robots over large obstacles using NMPC controller". *International Conference on Control, Instrumentation Automation*, Shiraz, Iran: IEEE, 2011, pp. 917-922.
39. Heydari, R., Farrokhi, M., "Robust model predictive control of biped robots with adaptive on-line gait generation". *International Journal of Control, Automation Systems*, 15, 2017, pp. 329-344.
40. Lawrynczuk, M., A family of model predictive control algorithms with artificial neural networks". *International Journal of Mathematics Computer Science*, 17, 2007, pp. 217-232.
41. Bigdeli, N., Afshar, K., Lame, B. I., Zohrabi, A., "Modeling of a five-link biped robot dynamics using neural networks". *Journal of Applied Science*, 8, 2008, pp. 3612-3620.
42. Prieto, A., Prieto, B., Ortigosa, E. M., Ros, E., Pelayo, F., Ortega, J., Rojas, I., "Neural networks: an overview of early research, current frameworks and new challenges". *Neurocomputing*, 214, 2016, pp. 242-268.
43. Westervelt, E., Grizzle, J. W., Chevallereau, C., Choi, J., Morris, B., "Feedback Control of Dynamic Bipedal Robot Locomotion (Automation and Control Engineering)". London: CRC Press, UK, 2007, pp. 205-389.
44. Bhounsule, P. A., "A controller design framework for bipedal robots: trajectory optimization and event-based stabilization". Doctoral Dissertation of University of Cornell, USA, 2012, pp. 43-89.